Chalcogenide Letters Vol. 6, No. 4, April 2009, p. 171 - 179

PREPARATION AND CHARACTERIZATION OF NANOCRYSTALLINE CdS THIN FILMS

M.THAMBIDURAI[a*], N.MURUGAN[b], N.MUTHUKUMARASAMY[a], S.VASANTHA[a], R. BALASUNDARAPRABHU[c], S.AGILAN[a]
[a]*Department of Physics, Coimbatore Institute of Technology, Coimbatore, India*
[b]*Department of Mechanical Engineering, Coimbatore Institute of Technology, Coimbatore, India*
[c]*Department of Physics, PSG College of Technology, Coimbatore, India*

CdS nanocrystalline thin films have been prepared by sol-gel spin coating method. CdS nanoparticle thin films have been prepared using cadmium nitrate as cadmium source and thiourea as sulfur source. The effect of annealing on the properties of the prepared CdS nanocrystalline films has been studied. The x-ray diffraction studies indicated the formation of nanocrystalline CdS thin films with hexagonal phase. The grain size has been found to lie in the range of 5 to 8.2 nm depending on the annealing temperature suggesting the formation of CdS quantum dots. These results have been confirmed using high resolution transmission electron microscope (HRTEM) analysis which also indicated the formation of nanocrystalline CdS with a grain size of nearly 5 nm. The absorption spectra demonstrated the presence of quantum confinement effect in the prepared CdS nanocrystalline films because of the small size of the particles. The photoluminescence spectra of the CdS films exhibited green and yellow emission bands.

(Received April 5, 2009; accepted April 16, 2009)

Keywords: Cadmium sulphide; Quantum dots; Electron microscopy (HRTEM); *S*emiconductors.

1. Introduction

CdS nanocrystalline thin films belonging to the cadmium chalcogenide family and used as window material for CdS/CdTe solar cells continues as a subject of intense research due to its potential application in solar cells. CdS with hexagonal structure is highly favorable for solar cell application as a window layer because of its suitable band gap and stability. CdS is one of the important material for application in electro-optic devices such as laser materials, transducers, photoconducting cells, photosensors, optical wave-guides and non-linear integrated optical devices [1]. The II–VI semiconductor nanocrystals exhibit interesting properties and their emission spectra is very narrow (spectrally pure) and the emission colour is simply tuned by changing their size. As the nanocrystal size decreases, the energy of the first excited state decreases qualitatively following a particle-in-a-box behaviour. This size dependence and the emergence of a discrete electronic structure from a continuum of levels in the valence and conduction bands of the bulk semiconductor result from quantum confinement; hence, semiconductor nanocrystals are referred to as quantum dots [2].

The use of polymers is a prominent method for the synthesis of semiconductor nanoparticles. The reason is that the polymer matrices offer advantages like easy processability, solubility and control of the growth and morphology of the nanoparticles. CdS nanoparticles embedded in different matrixes like polystyrene, polyvinyl alcohol, polyethylene glycol etc. have

* Corresponding author: vishnukutty2002@yahoo.co.in

been prepared by many workers [1-6]. CdS thin films have been prepared by different workers using various techniques such as electro deposition[7], screen printing[8], physical vapor deposition[9], spray pyrolysis[10], molecular beam epitaxy[11], chemical bath deposition[12], successive ionic layer adsorption and reaction[13], sonochemical[14] and spin coating method[15]. In comparison with the other techniques, sol-gel method is more suitable to prepare optical materials as it permits molecular-level mixing and processing of the raw materials and precursors at relatively lower temperature and produces nano-structured bulk, powders and thin films[16-18]. Sol-gel is a very attractive method to produce CdS films for photovoltaic applications for which large-area devices are required at low cost. It also does not limit the choice of the substrate material. In this paper, we report about the preparation of nanocrystalline CdS films using sol-gel spin coating method and also discuss the structural properties, surface morphology and optical properties of the prepared thin films.

2. Experimental

In the present study CdS particles have been embedded in polyethylene glycol based solution. A polyethylene glycol (PEG 400, Merck) sol was prepared by mixing 0.6 ml of PEG, with 8.9 ml of ethanol and 0.5 ml of acetic acid under stirring, which was continued for 1hour. Cadmium nitrate and thiourea were used as the precursors for incorporation of Cd and S respectively. These precursors were dissolved in ethanol with stirring. The as-prepared solution was slowly added to the PEG sol with vigorous stirring and was stirred for 5 - 6 hours to obtain the final sol ready for depositing thin films. The spin-coating technique was used to prepare thin films using the above sol on to glass substrates. The substrates were rotated at a speed of 500 rpm for 30 sec. After deposition, annealing of the sample is required for the removal of solvent and residual organics and film densification. So the films have been post-annealed in air at 150°C, 250°C, 350°C and 450°C.

X-ray diffraction studies have been carried out using PANalytical x-ray diffractometer, high resolution transmission electron microscope (HRTEM) images of the prepared CdS has been recorded using a Philips TECNAI F20 microscope, AFM measurements were performed on the sample by measuring the topography with a Digital instruments Dimension 3100 Scanning Probe Microscope operated in tapping mode. The optical properties have been studied using spectrophotometer (JASCO V-570) and the photoluminescence study has been carried out using Cary Eclise WinFLR photoluminescence device.

3. Results and discussion

The structural properties of the spin coated CdS films have been investigated by x-ray diffraction technique using CuK_{α} radiation. Figure 1 shows the x-ray diffraction pattern of CdS thin films prepared by spin coating method and annealed at 150°C, 250°C, 350°C and 450°C for 30 minutes. The x-ray diffraction pattern of 150, 250, and 350°C annealed samples exhibit peaks at 26.32° and 43.59° corresponding to the (002) and (110) directions. The diffraction pattern of CdS film annealed at 450°C exhibits two more additional peaks at 24.66 ° and 28.02° corresponding to (100) and (101) planes. As all these peaks correspond to the hexagonal phase, the prepared CdS films can be said to exhibit hexagonal phase. The lattice parameter values a and c have been calculated and are a = 4.41Å and c = 6.72 Å which are in agreement with the JCPDS data (41-1049). The presence of small peaks in the x-ray diffractogram reveals the formation of nanocrystalline CdS films. The peaks are not sharp indicating that the average crystallite size is small. Due to size effect the peaks in the

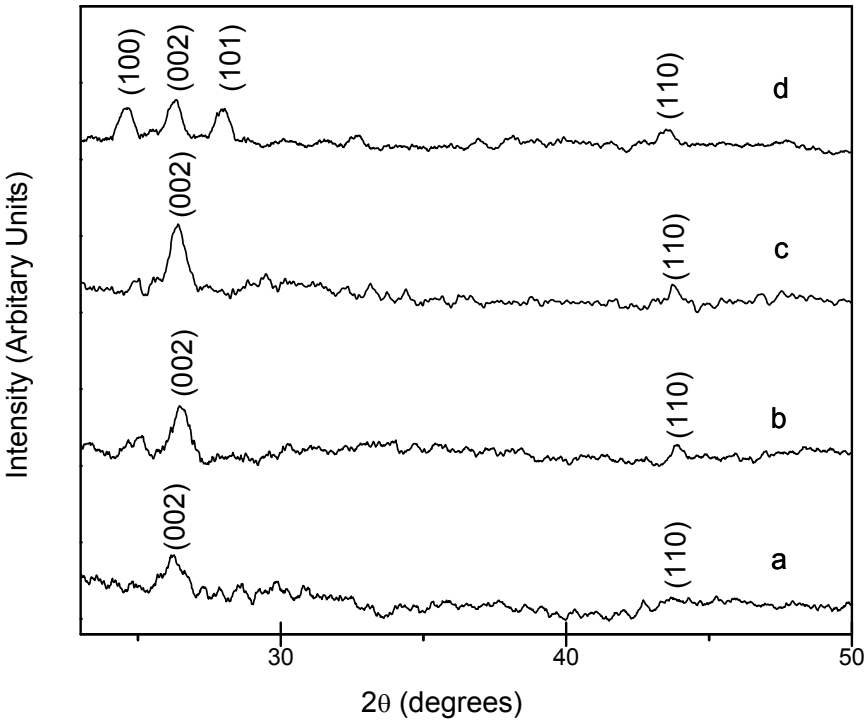

Fig. 1. X-ray diffraction pattern of CdS films annealed at different temperature (a) 150 °C (b) 250 °C (c) 350 °C d) 450 °C

diffraction pattern broaden and their widths become large as the particles become smaller. Crystallinity is found to improve with increase in annealing temperature.

The average size of grains has been obtained from the x-ray diffraction pattern using the Scherrer's formula [19]

$$D = \frac{k\lambda}{\beta \cos\theta}$$

where, D is the grain size, K is a constant taken to be 0.94, β is the full width at half maximum (FWHM) and λ is the wave length of the x-rays. The obtained grain size values of the annealed CdS films are given in Table 1. It is seen that crystallite size of CdS increases from 5 nm to 8.2 nm as the annealing temperature increased from 150 to 450°C. So it is found that nanocrystalline CdS films with particle size less than 10 nm has been prepared using the sol gel spin coating method. Figure 2 shows the high-resolution transmission electron microscopy (HRTEM) image of CdS nanocrystalline film annealed at a temperature of 150°C. The image (Figure 2a) clearly shows the lattice fringes indicating the formation of good nanocrystalline sample. The HRTEM image gives a grain size of ~ 5 nm and this is in agreement with x-ray diffraction results. This confirms the formation of nanocrystalline CdS films with particle size lying in the quantum dot range. The HRTEM image exhibits lattice fringes with d spacing of 0.357 nm corresponding to the (100) reflection of the hexagonal phase. Selected area electron diffraction (SAED) image (Figure 2b) exhibit diffraction rings corresponding to the (100), (110), (004), (105) and (213) directions of the hexagonal phase of CdS. The d spacing values obtained for all the diffraction rings from the SAED pattern match very well with that of hexagonal CdS. The appearance of multiple diffraction rings is due to the random orientation of the polycrystallites. The spotty ring pattern with missing periodicity observed in the SAED image is due to the fact that the films have random orientation.

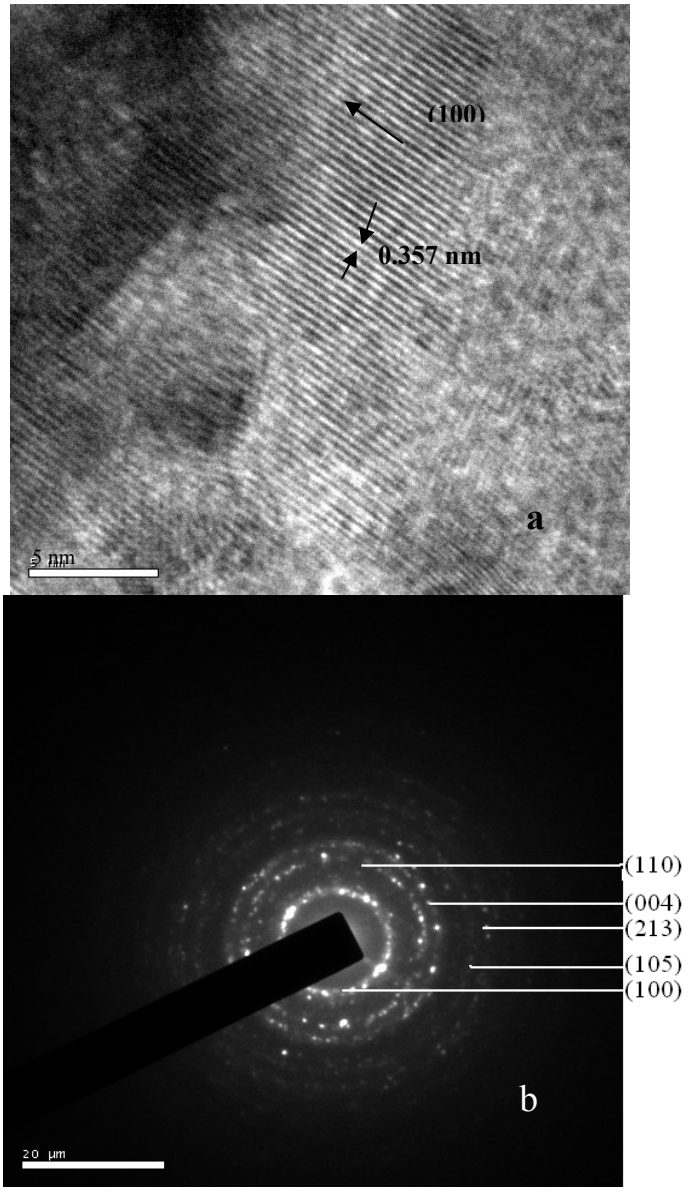

Fig. 2. High-resolution transmission electron microscopy and selected area electron diffraction images of CdS film annealed at 150°C.

Fig. 3 shows the AFM image of spin coated CdS thin film annealed at a temperature 150°C. The image shows well defined particle like features with granular morphology and indicates the presence of small crystalline grains. The root mean square surface roughness of the film is 37 nm. The image also reveals that the film is homogeneous without any cracks and is continuous with very well connected grains. The surface of most submicron particle is quite coarse and they are comprised of numerous nanoparticles with size ranging from 5 to 10 nm.

Due to the quantum size effects of nanoparticle semiconductors, UV-Vis spectroscopy has become an effective tool in determining the size and optical properties of the nanoparticles. Optical absorption spectra of CdS

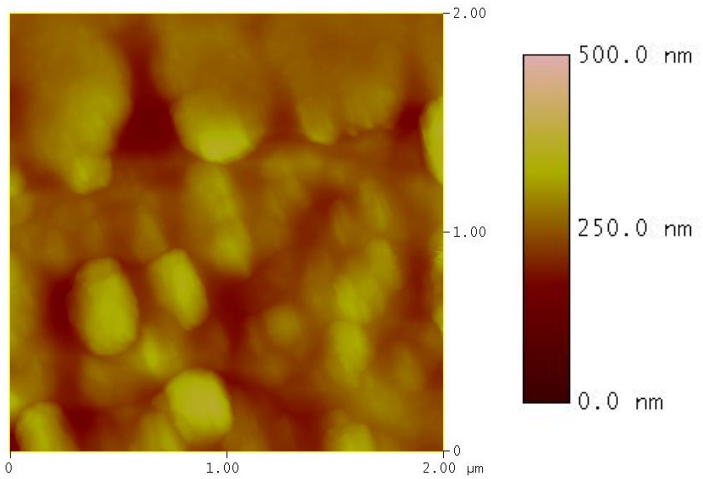

Fig. 3. AFM image of the CdS thin films annealed at 150°C

films annealed at different temperatures are shown in figure 4. As the size of the semiconductor particle decreases to the nanoscale the band gap of the semiconductor increases causing a blue shift in the UV-Vis absorption spectra. The bulk CdS material exhibits an absorption peak at about 515 nm. As the absorption peaks of the prepared CdS samples appear blue shifted compared with that of bulk CdS it can be easily understood that quantum confinement effect is present in the prepared CdS films. The gradual shift of absorption peaks towards longer wavelengths on increase in annealing temperature indicates the growth of the particles at higher temperatures.

The optical band gap has been calculated by plotting $(\alpha h\upsilon)^2$ versus $h\upsilon$(figure 5). By extrapolating the straight line portion of the curve to intercept the energy axis, the value of the band gap energy has been calculated. The calculated optical band gap values are found to be in the range 3.94 - 3.56 eV and are shown in Table 1.

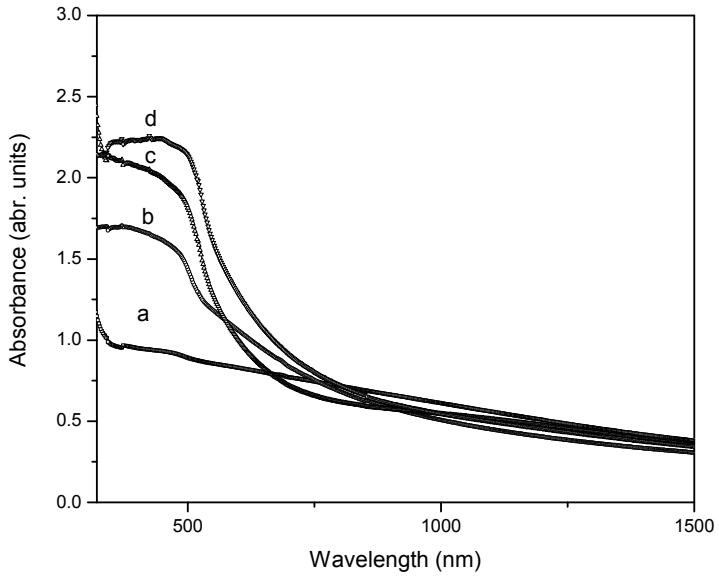

Fig. 4. Optical absorption spectra of annealed CdS films (a) 150 °C (b) 250 °C (c) 350 °C (d) 450 °C

The optical band gap obtained using the absorption spectra are greater than the bulk band gap (2.42 eV) and this indicates the formation of nanoparticles. On annealing the size of the

crystallite is found to increase resulting in decrease of band gap. The change in band gap with temperature

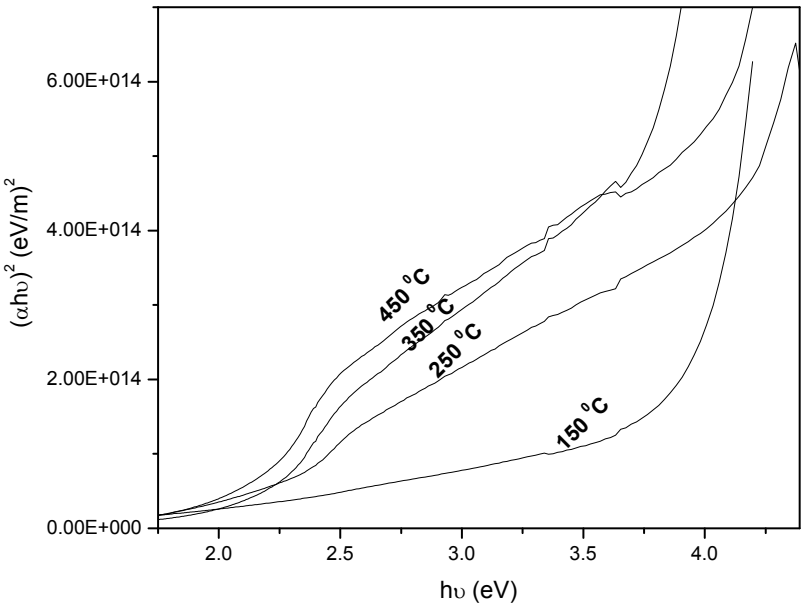

Fig. 5. Plot of $(\alpha h\upsilon)^2$ versus hυ of annealed CdS films

Table 1. Particle size from XRD and blue-shift of optical band gap (E_g) of CdS films annealed at different temperatures.

Annealing temperature(°C)	E_g (eV)	Particle size from blue-shift (nm)	Particle size from XRD (nm)
150	3.94	6.9	5.0
250	3.82	7.9	6.5
350	3.68	8.4	6.8
450	3.56	8.8	8.2

is attributed to quantum confinement effects [20]. The blue shift from 3.56 - 3.94 eV suggests strong quantum confinement. The band gap is found to decrease due to an increase of the cluster size or grain size(R); this is known as the quantum size effect. In the quantum size effect, both strong and weak confinements are possible, when $R << a_e$ the confinement is strong and it is weak for $R >> a_e$ where a_e is the effective Bohr radius and is 3.5 nm for CdS [21]. The strong and weak confinements occur due to the small and large grains in the sample. In general, a nanocrystalline sample is a combination of small and large grains. The expression for weak (E_w) and strong (E_s) confinement energies can be written as [22]

$$E_w = E_g + \frac{h^2\pi^2}{2MR^2}$$

$$E_s = E_g + \frac{h^2\pi^2}{2\mu R^2} - \frac{1.8e^2}{\varepsilon R}$$

where, E_g is the bulk band gap, $M = m_e^* + m_h^*$, μ reduced mass of exciton, the second term represents the kinetic energy of the confined exciton and the third term indicates the Coulomb interaction of the electron with the hole. Here coulomb interaction is negligible [22]. Even though the particle size obtained from x-ray diffraction results are found to be slightly larger than the Bohr radius of 3.5 nm for CdS, the strong confinement effect can be assumed to be prevalent in the prepared CdS nanocrystallline films because of the observed strong blue shift. Warnock and Awschalom[23] have reported strong confinement for CdSSe nanocrystals having grain sizes of 7.4 and 8.4 nm, even though the grain sizes were greater than the effective Bohr radius. The particle size has been calculated using the blue shift of the optical band gap caused by quantum confinement and is shown in Table 1. The particle size is found to lie in the range of 6.3 to 8.8 nm. These values are slightly different from the values obtained from x-ray diffraction studies. The particle size calculated from x-ray diffraction pattern are smaller than those calculated using absorption spectra and this may be due to the fact that the submicron particles are the aggregation of CdS nano particles.

Fig. 6 is the photoluminescence emission spectra of the annealed CdS nanoparticle thin films. PL spectra have been recorded at room temperature with an excitation wavelength of 400 nm. Emissions from semiconductor nanoparticles originate from electrons in the conduction band, excitonic states and trap states. It is important to note that any physical property that is dependent on the size of a quantum dot could also be used for predicting its size and distribution. It is well known that emission is very sensitive to nature of nanoparticle surface because of the presence of gap surface states arising from surface non stoichiometry and unsaturated bonds. Broad low energy spectrum is always attributed to trap state emission arising

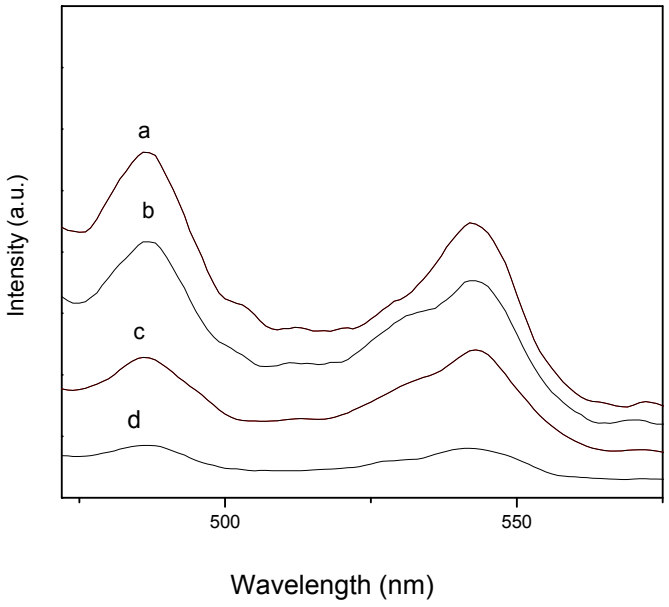

Fig. 6. Shows Photoluminescence emission spectra of annealed CdS (a) 150 °C (b) 250 °C (c) 350 °C (d) 450 °C.

from surface defects [24]. In CdS defects consists of cadmium vacancies, sulphur vacancies, interstitial cadmium and sulphur atoms adsorbed on the surface [25]. In the photoluminescence spectra the peak is found to broaden out with increase in annealing temperature. The inhomogeneous broadening of peaks can be attributed to high concentration of defects. The broadening of the peaks can be ascribed to the fact that large crystals tend to harbour more defects than small crystals. These defects may act as non-radiative recombination centres, which can quench the radiative band edge recombination [26]. The CdS emission spectra are also found to

increase in intensity with decrease in particle size i.e. with decrease in annealing temperature. In the nanocrystalline regime, since the number of molecules in the surface is more, surface defects play a vital role in determining the luminescence characteristics. In nanocrystals traps are more likely to be located at the surface. The smaller the particle diameter larger would be the surface area, leading to strong contribution from defect related luminescence emission.

The PL emission spectra of the spin coated CdS films shown in figure 6 is found to exhibit two emission peaks centred around 486 nm and 542 nm. The emission band present at 486 nm is known as green emission band of CdS. There are several explanations about the origin of green emission band in thin films. They may be due to i) recombination of free electrons from conduction band with holes captured on an acceptor level, ii) recombination of trapped electrons from a donor level with free holes and iii) recombination of electrons from a donor level with holes trapped on an acceptor level [27,28]. The green band emission in the present study may be due to the acceptor levels related to interstitial sulphur and donor levels due to native defects in the CdS lattice. The emission band at 542 nm is known as yellow band and is ascribed to the donor level of the interstitial cadmium atoms forming surface defects leading to trap emission in CdS. Similar results has been reported by earlier workers [29-31]. With decreasing size of the nanocrystallites, the density of the surface states would increase as a result of increase in surface to volume ratio. As a consequence of this increase in surface to volume ratio the luminescence is found to be dominated by surface state transitions rather than excitonic transitions.

4. Conclusions

Nanocrystalline CdS films have been prepared by sol-gel spin coating method. The x-ray diffraction and high resolution transmission electron microscope studies revealed the formation of small grains having a size of 5 to 8.2 nm depending on the annealing temperature resulting in the formation of CdS quantum dots. The absorption studies carried out on the prepared CdS films revealed a strong blue shift indicating the presence of quantum confinement effect. Photoluminescence spectra of the CdS films exhibited green and yellow band emissions corresponding to the defect related luminescence emission.

Acknowledgement

The authors thank the University Grants Commission, India for providing financial support.

References

[1] K. Senthil, D. Mangalaraj, S. K. Narayandass, Appl. Surf. Sci. **169/170,** 476 (2001).
[2] T. Kippeny, L. A. Swafford, S. J. Rosenthal, J. Chem. Edu. **79,** 1094 (2002).
[3] F. Antolini, M. Pentimalli, T. Di Luccio, R. Terzi, M. Schioppa, M. Re, L. Mirenghi, L. Tapfer, Mater. Lett. **59**, 3181 (2005).
[4] Hongmei Wang, Pengfei Fang, Zhe Chen, Shaojie Wang, Appl. Surf. Sci. **253,** 8495 (2007).
[5] J. X. Yao, G. L. Zhao, D. Wang, G. R. Han, Mater. Lett. **59,** 3652 (2005).
[6] D. Wu, X. Ge, Z. Zhang, M. Z. Wang, S. L. Zhang, Langmuir **20,** 5192 (2004).
[7] S. K. Das, Sol. Energy Mat. Sol. Cells **29,** 277 (1993).
[8] D. Patidar, R. Sharma, N. Jani, T. P. Sharma, N. S. Saxena. Bull. Mater. Sci. **29**, 21 (2006).
[9] R. W. Birkmire, B. E. McCandless, S. S. Hegedus, Solar Energy **12**, 45 (1992).
[10] P. Raji, C. Sanjeeviraja, K. Ramachandran, Bull. Mater. Sci. **28**, 233 (2005).
[11] J. W. Choi, A. Bhupathiraju, M. A. Hasan, J. M. Lannon, J. Cryst. Growth **255,** 1 (2004).
[12] Basudev Pradhan, Ashwani K.Sharma, Asim K. Ray, J. Cryst. Growth **304**, 388 (2007).
[13] Yashar Azizian Kalandaragh, M.B.Muradov, R.K.Mammedov, Ali Kaodayari, J.Cryst. Growth **305**, 175 (2007).

[14] V. P. Singh, R. S. Singh, G. W. Thompson, V. Jayaraman, S. Sanagapalli, V.K Rangari, Sol. Energy Mater. Sol. Cells **81**, 293 (2004).
[15] S.M.Reda, Acta Materialia **56**, 259 (2008).
[16] M. D.Curran, A.E.Stiegman, J. of Non-Cryst. Solids **249**, 62 (1999).
[17] H. X. Zhang, C. H. Kam, Y. Zhou, X. Q. Han, S. Buddhudu,Y. L. Lam, J. Opt. Mater. **15**, 47 (2000).
[18] T. Monde, H. Fukube, F. Nemoto, T. Yoko, T. Konakahara, J. Non-Cryst. Solids **246**, 54 (1999).
[19] M. Maleki, M. Sasani Ghamsari, Sh. Mirdamadi, R. Ghasemzadeh Semiconductor Physics – Quantum Electronics and Optoelectronics **10**, 30 (2007).
[20] N.N.Parvathy, G.M.Pajonk, A.V.Rao. J. Mater. Synth. Proc. **7**, 221 (1999).
[21] K. S. Ramaiah, A. K. Bhatnagar, R. D. Pilkington, A. E. Hillard, R. D.Tomlinson, J. Mater. Sci.: Mater. Elect. **11**, 269 (2000).
[22] B. K. Rai, H. D. Bist, R. S. Katiyar, M. T. S. Nair, P. K. Nair, A. Manivannan, J. Appl. Phys. **82**, 1310 (1997).
[23] J. Warnock, D. D. Awschalom, Physical Review B, **32,** 5529 (1985).
[24] E. Saunders, I. Popv, U. Banin, J. Phys. Chem. B **110**, 25421 (2006).
[25] J. Schroeder, P. D. Persans, T. G. Bilodeau, Physical Review B, **43,** 12580 (1991).
[26] N. Pinna, K. Weiss, J. Urban, M. Pileni, Advanced Materials (Weinhen, Ger.) **13,** 261 (2001).
[27] L. S. Pedrotti, D. C. Reynolds, Physical Review, **119**, 1897 (1960).
[28] B. A. Kulp, H. Kelley, J. Appl. Phys. **31**, 1057 (1960).
[29] M. Agata, H. Kurase, S. Hayashi, K. Yammamoto, Solid State Commun. **76,** 1061 (1990).
[30] M. Tata, S. Banerjee, V. T. John, Y. Waguespack, G. L McPherson, Colloid Surf. **A 27,** 39 (1997).
[31] S. Mandal, D. Rautaray, A. Sanyal, M. Sastry, J. Phys. Chem. B **108**, 7126 (2004).